Synergistic role of micronemal proteins in *Toxoplasma gondii* virulence

Odile Cérède,[1,2] Jean François Dubremetz,[2] Martine Soête,[3] Didier Deslée,[3] Henri Vial,[2] Daniel Bout,[1] and Maryse Lebrun[2]

[1]UMR Université-INRA d'Immunologie Parasitaires, Faculté des Sciences Pharmaceutiques et Biologiques, 37200 Tours, France
[2]UMR 5539 CNRS, Université de Montpellier 2, 34090 Montpellier, France
[3]FRE 2377 CNRS, Institut de Biologie de Lille, 59021 Lille, France

Apicomplexan parasites invade cells by a unique mechanism involving discharge of secretory vesicles called micronemes. Microneme proteins (MICs) include transmembrane and soluble proteins expressing different adhesive domains. Although the transmembrane protein TRAP and its homologues are thought to bridge cell surface receptors and the parasite submembranous motor, little is known about the function of other MICs. We have addressed the role of MIC1 and MIC3, two soluble adhesins of *Toxoplasma gondii*, in invasion and virulence. Single deletion of the *MIC1* gene decreased invasion in fibroblasts, whereas *MIC3* deletion had no effect either alone or in the mic1KO context. Individual disruption of *MIC1* or *MIC3* genes slightly reduced virulence in the mouse, whereas doubly depleted parasites were severely impaired in virulence and conferred protection against subsequent challenge. Single substitution of two critical amino acids in the chitin binding–like (CBL) domain of MIC3 abolished MIC3 binding to cells and generated the attenuated virulence phenotype. Our findings identify the CBL domain of MIC3 as a key player in toxoplasmosis and reveal the synergistic role of MICs in virulence, supporting the idea that parasites have evolved multiple ligand–receptor interactions to ensure invasion of different cells types during the course of infection.

CORRESPONDENCE
Maryse Lebrun:
maryse.lebrun@univ-montp2.fr

Abbreviations used: BHK, baby hamster kidney; CB, chitin binding; CBL, CB-like; HFF, human foreskin fibroblast; IF, immunofluorescence assay; MIC, microneme protein; ORF, open reading frame.

Apicomplexa are a group of mostly obligate intracellular parasites responsible for diseases such as toxoplasmosis, malaria, neosporosis, coccidiosis, and cryptosporidiosis. These parasites are polarized elongated cells that use a unique gliding motility mechanism to move on solid substates and penetrate host cell. Gliding and invasion depend on an actin–myosin system and on the release and capping of proteins from apical secretory vesicles named micronemes (for review see references 1 and 2). Microneme proteins (MICs) contain modules that are homologous to adhesive domains from higher eukaryotic proteins (3) and have often been shown to bind receptors on host cells. Upon secretion and redistribution on the parasite surface, transmembrane MICs are thought to connect external receptors to the submembranous acto–myosin motor that provides the power for parasite gliding and host cell invasion.

Recent works have provided molecular evidence that a transmembrane MIC protein conserved in a number of Apicomplexan genera (TRAP in *Plasmodium* and MIC2 in *Toxoplasma gondii*) is essential for both gliding and invasion. The adhesive modules of the ectodomain of TRAP are required for entry into a wide range of host cells, probably by interacting with several cell surface receptors or with an evolutionarily conserved cell surface receptor (4). The direct role of a specific tryptophan in the cytoplasmic tail of TRAP in the capping model has been obtained by reverse genetics (5) and its interaction with the actin binding protein aldolase has recently been demonstrated (6), unraveling a physical link between the transmembrane MICs and the subcortical motor. Most other MICs, including soluble proteins, also contain adhesive domains, which may act as additional components of the interaction of the parasite with the host cell surface and/or participate in the invasion of specific cells in the course of infection, although no demonstration of the function of these adhesins in virulence has been obtained so far.

The Apicomplexan parasite *T. gondii* is responsible for congenital infections in the developing fetus, severe neurological complications in immunocompromised individuals, and ocular

pathology in otherwise healthy individuals. In immunocompetent hosts, acute infection is generally benign and progresses rapidly into a chronic phase characterized by parasite encystment in various tissues, including the central nervous system and muscles. This opportunistic pathogen is able to infect and propagate in virtually all nucleated cells. Within its micronemes, a dozen of MICs have been characterized to date, among which the proteins MIC1 and MIC3 for which we have previously demonstrated host cell surface binding properties (7, 8). In this study, we have addressed, by genetic disruption, the role of these two adhesins in cell invasion and in toxoplasmosis.

MIC3 is a 90-kD soluble protein containing several epidermal growth factor–like domains and an NH_2-terminal chitin binding (CB)-like (CBL) domain, this latter being required for binding to host cells (9). In addition, binding re-

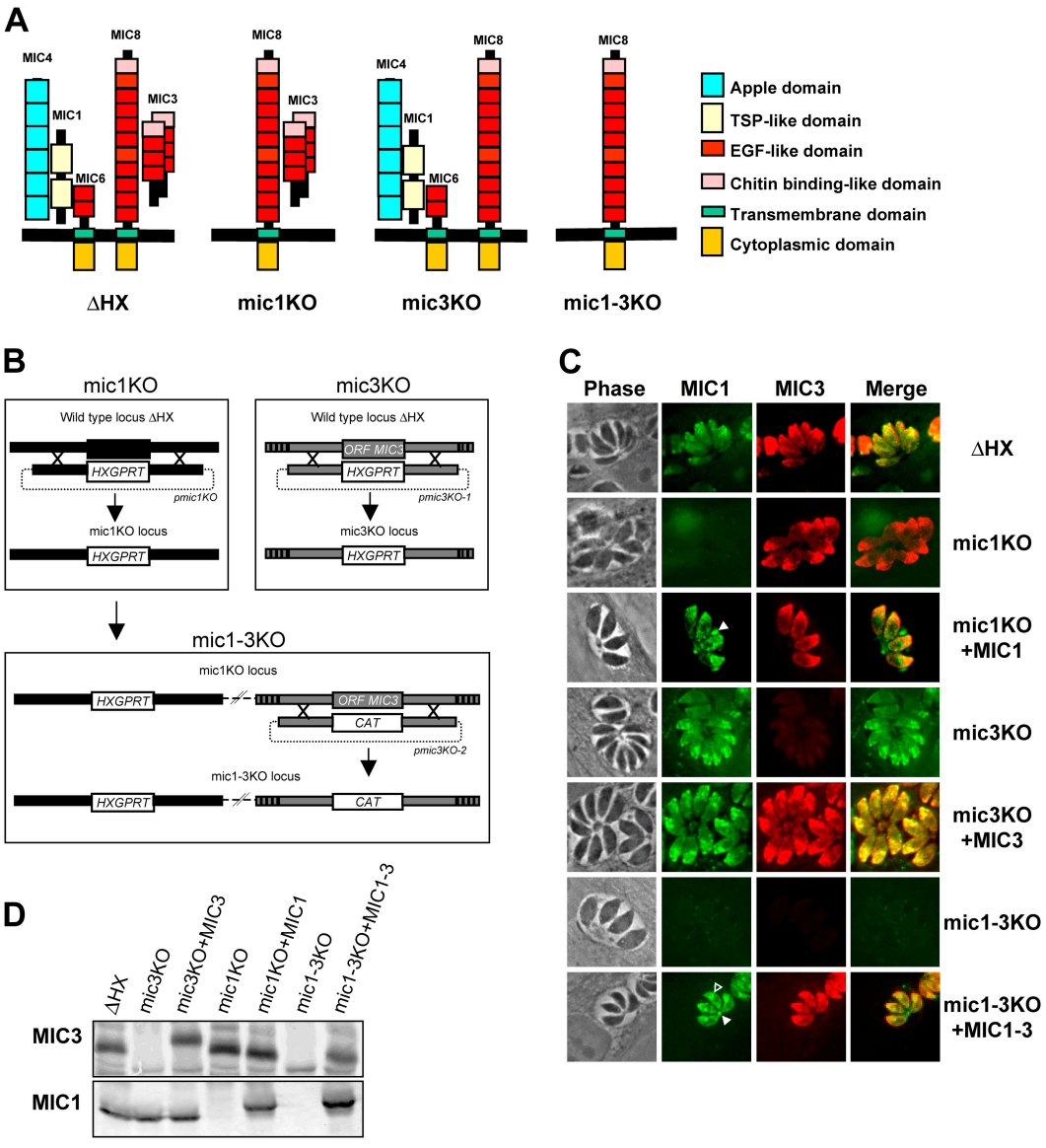

Figure 1. Disruption of *MIC1* and *MIC3* genes and genetic complementation. (A) Schematic representations of the MIC1/4/6 and MIC3/8 complexes in micronemes of the ΔHX strain and the KO strains constructed in this study. In mic1KO (and mic 1-3KO), MIC1 is ablated, whereas MIC4 and MIC6 are mistargeted, resulting in a triple deletion of the proteins in micronemes. (B) Schematic drawing of the KO procedures described in Results. (C) IF of ΔHX (wild-type), MIC KOs, and complemented parasites. In wild-type, polyclonal anti-MIC3 (red) and mAb anti-MIC1 (green) show a punctuate fluorescence pattern within the apical complex, characteristic of microneme staining. Anti-MIC1 does not label mic1KO and mic1-3KO, whereas mic3KO and mic1-3KO do not react with anti-MIC3. Reexpression of MIC3 in mic3KO and mic1-3KO fully restored microneme labeling, whereas reexpression of MIC1 in mic1KO+MIC1 and in mic1-3KO+MIC1-3 led to some parasitophorous vacuole (closed arrowhead) and perinuclear (open arrowhead) labeling in addition to microneme staining. (D) Western blot analysis of MIC1 and MIC3 expression. On the top, the membrane was probed with anti-MIC3, and on the bottom, it was probed with anti-MIC1. The mobility shift observed for MIC3 in mic3KO+MIC3 is consistent with the addition of the Ty-1 epitope tag in this strain. Note the mobility shift of MIC1 in both complemented strains due to the addition of an myc epitope tag.

quires dimerization of MIC3. A CB domain was first identified in wheat germ agglutinin, and then in a large number of other CB proteins of plant origin (10). Carbohydrate binding experiments did not reveal any interaction between MIC3 and *N*-acetyl-glucosamine, chitobiose, or chitotriose (unpublished data), suggesting a different specificity for this domain in MIC3. MIC3 is escorted to microneme by the transmembrane MIC8 (see Fig. 1 A; reference 11) and exocytosed and relocalized to the surface of the parasite during invasion (8).

MIC1 is also a soluble protein and contains a tandemly duplicated domain sharing distant homology with the TSP1-like domain of TRAP and has lactose binding specificity (12). MIC1 assembles with MIC4 and MIC6 (11, 13), and the transmembrane protein MIC6 functions as escorter to target the soluble proteins MIC1/4 to the micronemes (see Fig. 1 A). A MIC1 KO parasite (mic1KO) and the complemented strain (mic1KO+MIC1) were generated previously (13). The absence of MIC1 was shown to exert a drastic and specific effect on the sorting of MIC4/6, but its impact on cell invasion has not been investigated.

In this study, we show that deletion of MIC1 decreases the invasion of human fibroblasts and that MIC1 and MIC3 perform complementary functions in *T. gondii* virulence in mice. Furthermore, we demonstrate that virulence in mice requires the binding capability of the MIC3 CBL domain, this latter depending on critical aromatic amino acids.

RESULTS

Targeted disruption of the *MIC3* gene and complementation of the KO parasite

The *MIC3* gene that is present as a single copy in the haploid genome of *T. gondii* (8) has been disrupted by homologous recombination (Fig. 1 B, right). On immunofluorescence assay (IF) of intracellular mic3KO tachyzoites (Fig. 1 C) or Western blots of parasite extracts (Fig. 1 D), no MIC3 protein could be detected. Loss of the *MIC3* gene was confirmed by Southern blot analysis with a MIC3-specific probe (not depicted). Complementation of the mic3KO clone with plasmids pM3MIC3ty and pTUB/CAT generated a mic3KO+MIC3 clone. Southern hybridizations revealed that both pM3MIC3ty and pCAT were integrated as single copies into the genome (not depicted). Wild-type–like reexpression of MIC3ty in complemented parasites was shown by IF (Fig. 1 C) and Western blotting (Fig. 1 D). Dimerization and processing of MIC3, which conditioned the binding properties of the protein (9), were confirmed by Western blot (not depicted). As the absence of soluble MICs has been shown to exert a drastic and specific effect on the sorting of the other members of micronemal complexes (13, 14), we analyzed the localization of MIC8, which is the escorter of MIC3, in the mic3KO. We found that the expression level and the trafficking of MIC8 to micronemes was not affected in the absence of MIC3 (not depicted). In addition, MIC1, MIC2, MIC4, MIC6, and MIC10 all showed normal localization to micronemes in this mutant.

Mic1KO parasites are defective in invasion

We then tested the ability of mic1KO and mic3KO tachyzoites to invade and replicate in human foreskin fibroblasts (HFFs). Remarkably, the invasion rate of mic1KO parasites was decreased by ~50% relative to wild-type ΔHX, whereas the mic3KO invaded cells as the control (Fig. 2 A). No change in replication rate was observed (not depicted). Complementation of mic1KO by MIC1 significantly restored invasion competence. However, complete rescue was never obtained, which may result from the partial missorting of MIC1 in this strain. Indeed, a small proportion of MIC1myc reached the parasitophorous vacuole as described previously (13), and a diffuse juxtanuclear staining was also observed, likely representing ER/Golgi retention (Fig. 1 C). As a decrease in invasion could arise from (a) a defect in gliding motility, (b) a reduction in cell attachment, or (c) a reduction of penetration without attachment defect, we performed additional experiments. Gliding motility was analyzed using time-lapse video microscopy. No significant difference was found between ΔHX and mic1KO parasites (2.1 ± 0.4 μm/s and 1.8 ± 0.3 μm/s, respectively). To quantify attachment versus penetration, a red/green assay was used (14). This allows one to distinguish extracellular and attached parasites from invaded parasites. As shown in Fig. 2 B, no significant decrease in attachment was observed for mic1KO compared with the parental strain, whereas the defect in invasion was again evidenced. In addition, the same defect was observed at 15 min of invasion (Fig. 2 B), 30 min (not depicted), or longer times such as 6 (not depicted) and 12 h (Fig. 2 A), suggesting that the difference between ΔHX and mic1KO parasites is more likely to arise from a true defect in invasion rather than from a lower extracellular viability of the mutant parasites. In the case of mic3KO, a red/green assay performed at 15, 30, and 60 min (not depicted) did not show any significant difference with the wild-type, therefore excluding a more subtle defect such as a delay in invasion that might have been missed in the long-term invasion assay shown in Fig. 2 A.

Collectively, these results demonstrated that MIC3 deletion has no impact in invasion of HFFs, whereas the deletion of the *MIC1* gene affects the invasion capability of the parasite without affecting gliding motility nor cell adhesion.

Individual disruptions of *MIC1* and *MIC3* genes do not dramatically impair parasite virulence in mice

We then tested the virulence of mic1KO and mic3KO in vivo in a mouse model. All of the parasites used in this study (ΔHX, KO, and complemented) were of the RH strain, a type 1 strain, which typically kills mice 7–10 d after i.p. infection with a single tachyzoite (see Discussion). In our experiments, all mice died within 9 d after i.p. injection with 20 ΔHX tachyzoites (Fig. 2 C). Mice infected with mic1KO or mic3KO died between days 9 and 22 after infection. One mouse infected with mic3KO was still alive after 40 d, and this animal had developed a *T. gondii* B cell–specific response, as determined by immunoblot (not depicted). This slight delay in killing was observed in two independent experiments and reverted after complementation (Fig. 2 C).

This indicated that the lack of *MIC1* or *MIC3* genes slightly decreases virulence in mice.

Double disruption of *MIC1* and *MIC3* genes and invasion phenotype of the mutant

Both mic1KO and mic3KO mutants were still able to invade cells and kill mice, consistent with the idea that *T. gondii* has evolved multiple ligand–receptor interactions to invade cells in the course of infection. We speculated that simultaneous disruption of multiple ligand–receptor systems would be deleterious to the parasite. To address this issue, we deleted the *MIC3* gene in the mic1KO mutant (Fig. 1 B). Western blotting and IF confirmed the absence of expression of MIC1 and MIC3 in the mic1-3KO clone (Fig. 1, C and D). Southern blot experiments confirmed the loss of *MIC3* gene in mic1-3KO (not depicted). Reexpression of both proteins was obtained in the complemented strain named mic1-3KO+MIC1-3 (Fig. 1, C and D). A small proportion of MIC1myc was retained in RE/Golgi or delivered in the parasitophorous vacuole, like in mic1KO+MIC1.

Next, we tested the impact of *MIC1* plus *MIC3* gene loss on HFF invasion. Double *MIC1* and *MIC3* deletion resulted in an invasion defect that was not significantly different from single MIC1 KO (Fig. 2 A), indicating that MIC1 and MIC3 have no additive function in fibroblast invasion in vitro and that the wild-type invasion phenotype of the mic3KO was not due to compensation by MIC1.

Parasites depleted in both *MIC1* and *MIC3* are markedly impaired in virulence and confer protection against *T. gondii* challenge

We then tested the impact of simultaneous disruption of MIC1 and MIC3 genes on mouse infection, as described above. Spectacularly, our experiments showed that 9 out of 10 mic1-3KO–infected mice survived the assay (Fig. 2 C), and the one that died did so 10 d later than those infected with the ΔHX control strain. Western blot analysis confirmed seroconversion of the surviving mice. The phenotype observed resulted effectively from loss of *MIC1* and *MIC3* genes because complementation of mic1-3KO with both

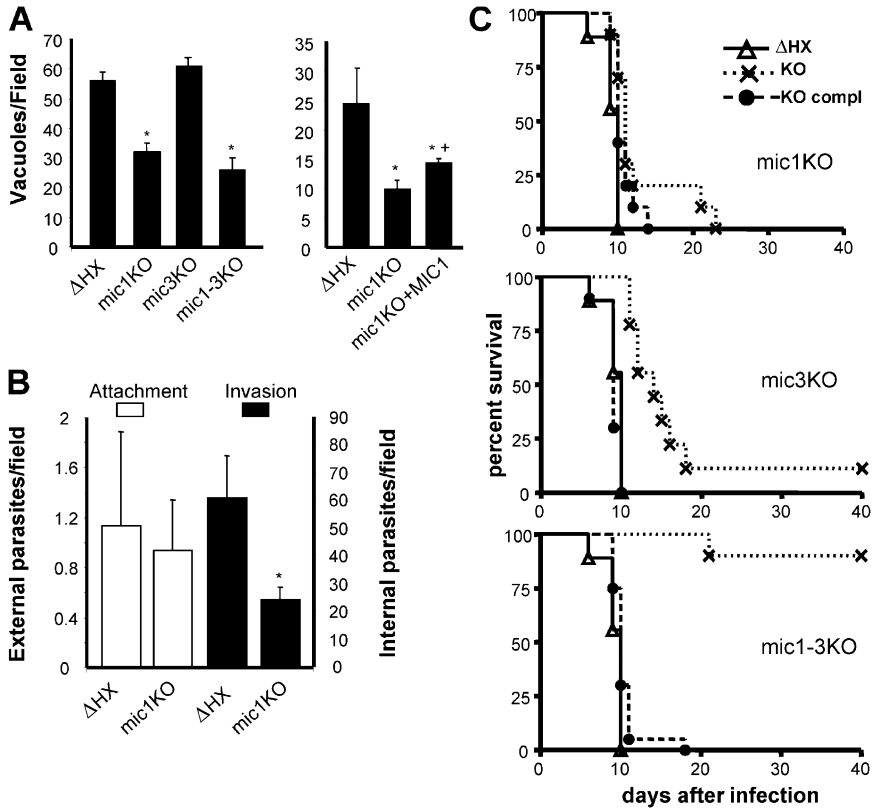

Figure 2. Phenotypes of MIC KO parasites. (A) Deletion of the *MIC1* gene reduces invasion in HFF cells. Confluent monolayers of HFF cells were incubated with tachyzoites, and invasion was assessed as described in Materials and methods. Results are presented as the number of vacuoles per field. Data are mean values ± SEM determined by quadruple assays (10 fields per assay) performed in five separate experiments. Asterisk and cross indicate a significant difference ($P < 0.05$, two-tailed Student's *t* test) compared with ΔHX and mic1KO, respectively. (B) Differentiation of invaded parasites from attached parasites with a red/green invasion assay. Data are mean values ± SEM of parasites by field determined by triplicate assay (10 fields per assay) performed in four separate experiments. The asterisk indicates a statistically significant difference compared with ΔHX. (C) Single deletion of *MIC1* or *MIC3* gene slightly reduced virulence in mice, whereas the double KO severely impaired virulence. 20 tachyzoites of the indicated strains were injected i.p. into OF1 male mice ($n = 10$), and mouse survival was monitored daily for 40 d. The mic1KO, mic3KO, and mic1-3KO were statistically less virulent than wild-type ($P < 0.002$, $P < 0.0001$, and $P < 0.0001$, respectively, by Logrank test), and the double deletion significantly reduced the virulence compared with the single deletion ($P < 0.0001$).

MIC1 and *MIC3* restored parasite virulence. In addition, we infected mice with different doses of mic1-3KO and compared the lethal dose (LD_{100}) with that of the parental strain. The LD_{100} of ΔHX at 9 d was <20 parasites, whereas that of the mic1-3KO was in the order of 2×10^3 parasites. Taken together, these results show that single deletions of the *MIC1* or *MIC3* gene do not have a dramatic impact on the outcome of mouse infection, whereas a double *MIC1* plus *MIC3* deletion markedly impairs virulence, demonstrating that MICs play a synergistic role in *T. gondii* virulence.

The asexual life cycle of *T. gondii* comprises two successive stages: the rapidly dividing tachyzoites, which disseminate in the host, and the slowly dividing bradyzoites, which encyst in the brain and other tissues (latent infection) and can assure transmission when an animal ingests bradyzoite-infected tissue. The mic1-3KO–surviving mice did not develop any infectious brain cyst, as expected for RH parasites that have lost the ability to make bradyzoites. Therefore, we studied the protection afforded by the mic1-3KO by infecting the mic1-3KO–surviving mice with a cyst-forming strain (76K) and counting the brain cysts arising after this challenge. Eight control mice orally infected with 76K bradyzoites (20 cysts) developed heavy cyst burdens at 1 mo after infection, averaging 4,000 per brain. Remarkably, in eight of the nine mice preinfected with mic1-3KO and challenged with the 76K strain, we could not detect any cyst. Only one mouse showed a few cysts (~30 in the total brain). These data demonstrate that mic1-3KO parasites were highly effective in inducing protective immunity in mice.

The CBL domain–mediated cell binding of MIC3 is crucial for expression of virulence

We have previously shown that MIC3 possesses a strong affinity for the host cell surface, essentially mediated by the CBL domain (8, 9). Therefore, discovering that *MIC3* gene disruption did not change the fibroblast invasion capability in vitro, although it was involved in decreased virulence, was surprising. Thus, we hypothesized that either other MICs may have compensated for this deletion in vitro (whereas in vivo, the cell binding function of MIC3 is critical for virulence) in association with the MIC1/4/6 complex, or the function of MIC3 in virulence is independent of its interac-

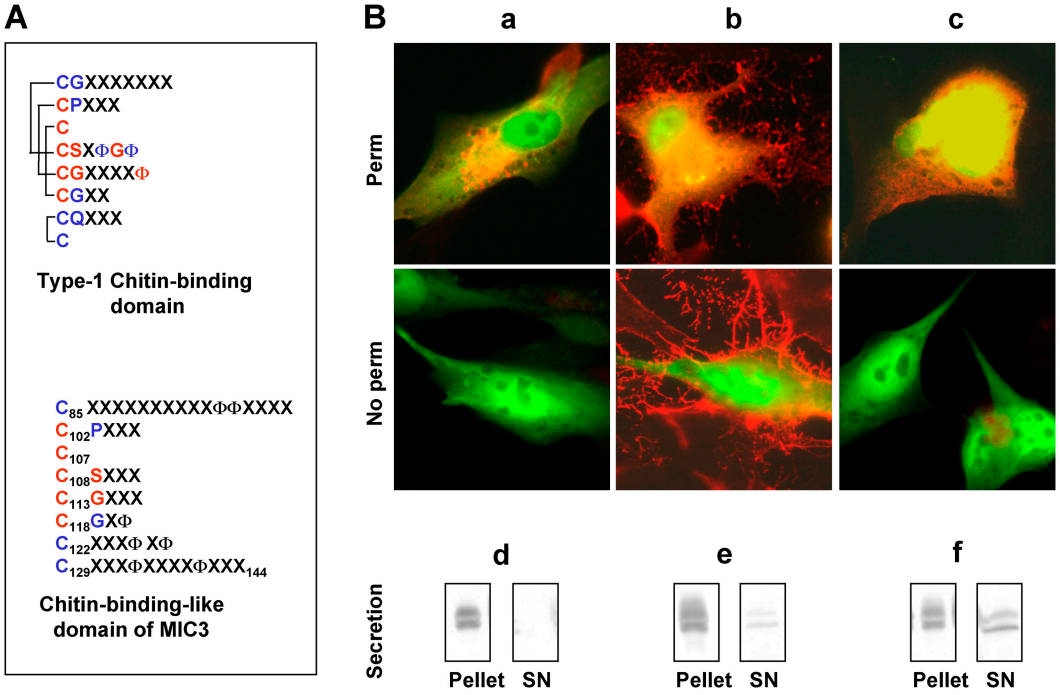

Figure 3. Identification of critical residues in the CBL domain of MIC3. (A) Representation of conserved residues in the CB type 1 domain (PROSITE PDOC00025, CB type 1 domain signature and profile) and the CBL domain of *T. gondii* MIC3 (CAB56644). The topological arrangement of the four disulfide bonds is indicated by brackets. Conserved residues of the binding site are in red letters and well-conserved positions are in blue letters. C, cysteine; S, serine; P, proline; X, any amino acid; Φ, aromatic amino acid. All amino acids are contiguous, but the sequences are represented with a carriage return before each cysteine. (B) IF of mutated MIC3 proteins in transfected cells. BHK-21 cells were transfected with plasmids allowing expression of MIC3 or mutated MIC3 tagged with V5 epitope and coexpression of the green fluorescent protein. Cytoplasmic fluorescence of green fluorescent protein allows the monitoring of transfected cells. MIC3 was visualized with mAb anti-V5 (red) after permeabilization (Perm, intracellular MIC3) or without permeabilization (No perm, surface-bound MIC 3). Secretion was monitored by Western blotting. (d, e, and f). Equivalent fractions of cells (pellet) and corresponding supernatants (SN) collected 18 h after transfection were probed with mAb anti-V5. Three phenotypes were obtained: the recombinant protein is retained in the secretory pathway (exemplified by Y141 in a and d); the protein is secreted and binds to the surface of transfected cells (exemplified by R-MIC3 in b and e); and the protein is secreted but does not bind to the surface of transfected cells (exemplified by F128A in c and f). Adhesive proteins show a stronger signal in the pellet, resulting from their surface association, in contrast to nonadhesive R-MIC3 where a stronger signal is obtained in the supernatant.

tion with the host cell surface. Therefore, we decided to construct parasites selectively defective for the MIC3-mediated adhesive function. We first dissected the CBL domain of MIC3 to identify amino acids critical for binding.

The CB consensus includes eight disulfide-linked cysteines and several highly conserved aromatic residues (Fig. 3 A). The cysteines have been shown to ensure proper protein folding, and the aromatic residues have been shown to interact with *N*-acetyl-glucosamine (15). Interestingly, in the CBL domain of MIC3, the position of the cysteines is conserved and numerous aromatic residues are present, although not positioned as in the consensus sequence (Fig. 3 A), which may explain the different specificity for this domain in MIC3. We then identified critical residues involved in cell surface binding by substituting individually three cysteines and all of the aromatic residues in the CBL domain of MIC3 and by analyzing the variant proteins for their binding properties by expression in mammalian cells, as described previously (9). The constructs were therefore transfected in baby hamster kidney (BHK)-21 cells, and the binding properties of recombinant MIC3 (R-MIC3) were analyzed by immunodetection on the cell surface and in the culture supernatant. Under these experimental conditions, native MIC3 has been shown to bind cell surface upon secretion by transfected cells, whereas CBL domain–depleted MIC3 was released in the supernatant (9). The correct dimerization of all the R-MIC3 was demonstrated by Western blot under unreducing conditions (not depicted). All cysteine to glycine substitutions (C102G, C107G, and C108G) led to a major defect in secretion and accumulation of the R-MIC3 in large perinuclear vesicles (an example is shown in Fig. 3 B, a and d), suggesting that cysteines ensure proper folding of the domain. In aromatic residue-substitution experiments, mutations F121A and Y141A also affected routing of the proteins in the secretory pathway of BHK-21 cells. The possible contribution of F121 and Y141 in binding properties could therefore not be analyzed this way. All other

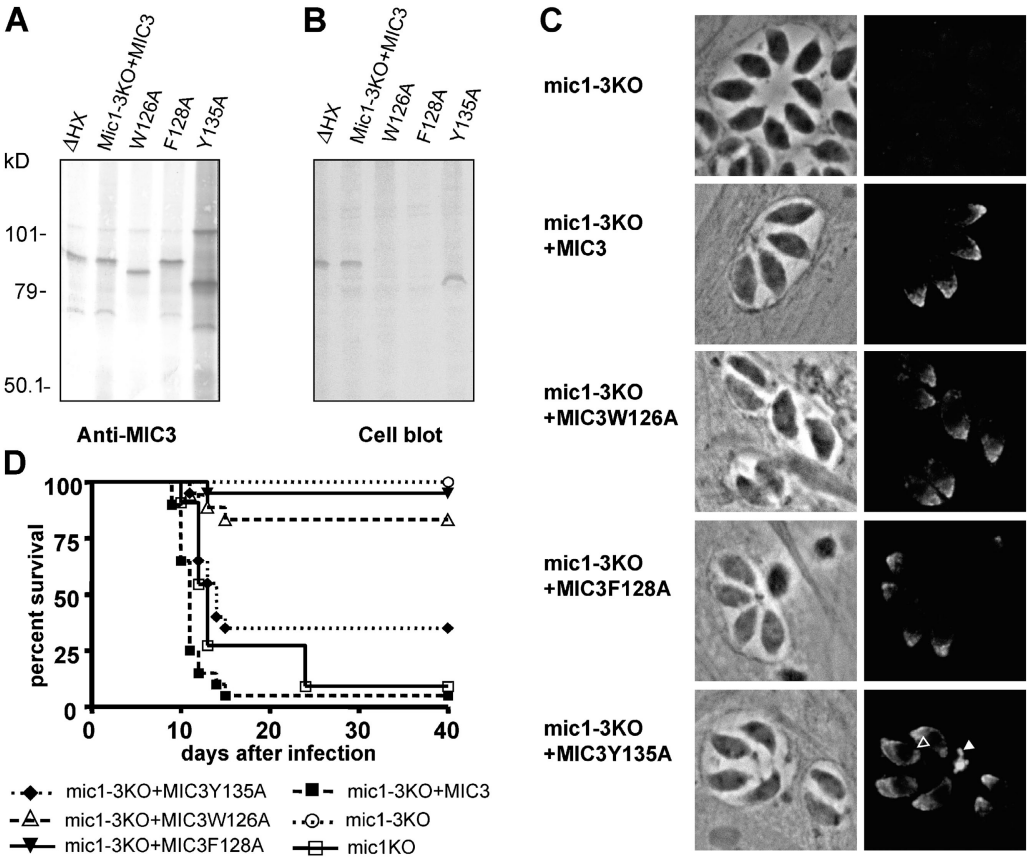

Figure 4. The cell binding property of MIC3 is crucial for virulence. Single amino acid mutations were generated in the *MIC3* gene and transfected in the mic1-3KO mutant. (A) Western blot of transgenic parasites under nonreducing conditions. The nitrocellulose membrane was probed with mAb anti-MIC3. (B) Cell blot analysis of transgenic parasites. A duplicate nitrocellulose membrane was incubated with Mode-K cells, washed, and bound cells were stained with amidoblack. Cells do not bind to W126A and F128A. (C) Phase contrast and IF of intracellular tachyzoites showing expression and microneme localization of MIC3 in the single amino acid mutants. Y135A in mic1-3KO also accumulates in the parasitophorous vacuole (closed arrowhead) and in the perinuclear area (open arrowhead). (D) Virulence of transgenic parasites. 20 tachyzoites of the indicated strains were injected i.p. into OF1 male mice ($n = 20$) that were monitored for 42 d. The mic1-3KO and the mutants complemented with W126A and F128A are markedly impaired in virulence and were not statistically different from mic1-3KO (Logrank test), whereas complementation with MIC3 or Y135A restored totally or partially the mic1KO phenotype. Mic1-3KO+MIC3Y135A was statistically more virulent than mic1-3KO ($P < 0.0009$) but was significantly less virulent than mic1-3KO+MIC3 ($P < 0.0001$).

R-MIC3s (Y96A, F97A, P103A, W126A, F128A, and Y135A) were secreted (Fig. 3 B, e and f). Two of them, W126A and Y128A, did not bind to the surface of transfected BHK-21 cells (Fig. 3 B, c). Consistent with the loss of their binding properties, they were abundantly secreted in the supernatant (Fig. 3 B, f). Taken together, these results show that single replacements of W126 or Y128 resulted in complete loss of binding function, suggesting that they are involved in interaction with the host cell receptor.

We then constructed parasites in which the CBL domain of MIC3 had lost adhesive function to test their virulence in vivo. Clones mic1-3KO+MIC3W126A and mic1-3KO+MIC3F128A expressed MIC3 with substituted tryptophane 126 and phenylalanine 128, respectively. Clone mic1-3KO+MIC3 expressing wild-type MIC3 and clone mic1-3KO+MIC3Y135A expressing MIC3 with a substituted tyrosine 135, which does not modify binding, were used as positive controls for binding. Southern blot experiments showed that only one copy of the MIC3 sequence was inserted in the genome of each of the complemented strains (not depicted). Western blotting and IF confirmed the restoration of protein expression and microneme targeting, except that Y135A was also partly retained in RE/Golgi or secreted in the vacuolar space (Fig. 4, A and C). All mutated MIC3 migrated at the size expected for a dimer under unreducing conditions (Fig. 4 A) and were correctly processed (not depicted). However, W126A and Y135A migrated faster than the others. This difference was also observed in mammalian cells and was not seen in reduced conditions (not depicted), indicating that this resulted from a modification of conformation. Binding properties of the proteins were analyzed by cell blot analysis. In brief, parasite lysates were separated by SDS-PAGE and transferred onto a nitrocellulose sheet, which was then incubated with a suspension of mammalian Mode-K cells. As expected, the cells bound strongly to endogenous MIC3 (Fig. 4 B, lane 1), transgenic MIC3 (lane 2), and Y135A (lane 5). In contrast, cells were unable to bind to W126A and F128A (Fig. 4 B, lanes 3 and 4). Interestingly, like in mammalian cells, the conformation change in Y135 did not affect its binding properties. Semiquantitative analysis on Western blots indicated that all variants were produced at levels similar to wild-type (not depicted). Taken together, these results showed that these transgenic parasites were suitable for analysis of the implication of MIC3 binding in virulence in mice.

As expected, mic1-3KO parasites complemented with the *MIC3* gene–killed mice as mic1KO controls (Fig. 4 D). When mic1-3KO parasites transfected with MIC3W126A or MIC3F128A were used to infect mice, we observed 83.3 and 95% of survival at 40 d after infection, respectively. In contrast, reexpression of MIC3Y135A in the mic1-3KO largely rescued the defect in virulence in mice, although not completely. This might be due to partial missorting of the Y135A protein.

Collectively, these results demonstrate that the binding property of the CBL domain of MIC3 is crucial for parasite virulence.

DISCUSSION

A large number of transmembrane and soluble MICs with adhesive properties have been identified in Apicomplexa-invasive stages. To date, a dozen of MICs, among which are three heteromeric complexes (MIC2/M2AP, MIC1/4/6, and MIC3/8), have been described in *T. gondii*. Several results indicate that the MIC2/M2AP complex plays a pivotal role in invasion, whereas little is known about the contribution of the other MICs in this process and in *T. gondii* virulence, except a decrease in invasion in the presence of anti-AMA1 antibodies (16). Here, we demonstrate by genetic disruption that other MICs contribute to the invasion of *T. gondii* in vitro and show for the first time the essential role played by MICs in *T. gondii* virulence in vivo. Indeed, most of the studies so far have investigated the function of MICs in host cell invasion in vitro. Our work shows that the importance of MIC is better evaluated in vivo than in vitro. Indeed, motility, adhesion, and invasion, which are the functions postulated for MIC proteins, are multifactorial phenomena, the expression of which is likely to differ in vivo from what occurs in the static environment found in a culture dish.

Efficient invasion is sustained by multiple ligand–receptor interactions

Most invasive-stage Apicomplexan parasites are highly motile and move on cells or substrates before penetrating a host cell. Both phenomena are thought to result from surface capping of transmembrane MICs, which link the substrate to the submembranous motor of the parasite. Gliding requires the rapid formation and breakage of interactions between the organism and the substrate, whereas penetration involves the formation of a tight association between the parasite and the cell (the moving junction), which moves backward over the parasite surface and through which the parasite exerts the traction required to enter the cell. The molecular interactions are likely quite different between the two processes. Collectively, our results show that the presence of MIC1/3/4/6 in micronemes is not required for motility, indicating that at least some of the MICs are dispensable for this process. In contrast, the deletion of the *MIC1* gene reduced invasion. Because *MIC1* deletion also results in defective targeting of both MIC4 and MIC6 in micronemes (13), this defect in invasion can be assigned to the absence of the MIC1/4/6 complex, without further precision. The residual invasion of the mic1KO parasites in fibroblasts is not due to MIC3 because double *MIC1* and *MIC3* deletion resulted in an invasion defect that was not significantly different from single MIC1 KO, but is certainly due at least in part to the MIC2/M2AP complex that has previously been described to be involved also in invasion of HFFs (14). Repeated attempts to disrupt the gene encoding MIC2 were unsuccessful (14), suggesting that similar to TRAP in *Plasmodium* sporozoites, MIC2 (the homologue of TRAP) is an essential protein. Therefore, one can suggest that accessory MICs participate in the complex puzzle of penetration where TRAP

homologues are certainly one of the major pieces. A basal affinity supplied by MIC2 receptor interaction and completed or stabilized by other MIC receptor interactions such as by MIC1/4/6 in HFFs can therefore be proposed to explain the efficient and/or ubiquitous invasiveness of *T. gondii*. In addition, our data suggest that the impact of MICs in the efficiency of invasion is likely to be driven by their involvement in the establishment of the most appropriate moving junction in a given cell type, the molecular composition of which is likely to differ depending on the cell type invaded.

MIC1 and MIC4 are soluble proteins containing adhesive modules and are associated with the transmembrane MIC6 protein. MIC6 shares with TRAP-MIC2 a sub–C-terminal tryptophan involved in the case of TRAP-MIC2 in gliding motility/invasion by linking the transmembrane protein to the submembranous motor (5, 6). Both MIC1 and MIC4 bind host cell in vitro; however, no binding properties have been described for MIC6 (7, 17). Therefore, MIC6 might anchor the two other proteins and interact with the underlying motor, whereas MIC1/MIC4 would establish specific interactions with host cell receptors involved in stabilizing the moving junction. The respective part of each partner of the complex will require complementary studies.

Our study shows that *MIC3* deletion does not modify invasion in HFFs. This was surprising because we had previously shown that MIC3 is rapidly redistributed toward the posterior pole of the parasite during invasion and that MIC3 was able to bind to a wide variety of cell types, including fibroblasts, macrophages, and epithelial cells (8). One explanation is that the large repertoire of MICs recognizes different receptors to ensure invasion of different cells and that in some cells, like HFFs, MICs may have redundant functions, whereas in others some could be crucial depending on the nature and abundance of receptors present. Complexity is added by the fact that parasites might be able to use alternative pathways for invasion, as first revealed by the deletion of the EBA-175 gene in *Plasmodium falciparum* (18). Functional inactivation of one gene may force switching or up-regulation of other MICs to allow survival of the parasites in vitro. Finally, even if this switch does not change the rate of invasion in vitro, loss of one pathway would be disadvantageous in natural infection.

MICs play a synergistic role in virulence

Toxoplasmosis begins with a brief acute phase followed by an asymptomatic chronic infection. In the highly susceptible mouse, infection by one parasite of the RH strain, the strain used in this study, is characterized by a rapid dissemination of the parasite to the lungs between days 2 and 4 after infection, and then to the brain at day 6, leading to death by pneumonia or encephalitis (19). A prerequisite for colonization of the organs by *T. gondii* is the invasion of cells. Because disruption of the *MIC1* gene substantially impaired invasion of fibroblast in vitro, the slight decrease in virulence observed for the mic1KO parasites was not surprising. Mic3KO parasites also showed a death delay in mice, even though no effect was observed in vitro. Consistent with this, MIC3 could be essential for invading specific cell types other than those that have been tested thus far. This hypothesis is supported by our demonstration that the binding ability of MIC3 to host cells is crucial for parasite virulence. More spectacular was the considerable decrease in virulence in vivo observed by simultaneous disruption of the *MIC1* and *MIC3* genes. This result demonstrates that MICs have a synergistic effect on infection in vivo and underline the difficulty in extrapolating in vitro data to the in vivo situation. The function of MICs in attachment/invasion may thus be more clearly revealed in dynamic conditions.

The outcome of acute toxoplasmosis in the mouse model is strongly dependent on the genotype of the parasite. Type I strains are typified by their extreme virulence in the murine host, where infection with a single parasite leads to death. In contrast, type II and III strains have a LD_{100} of $\geq 10^3$ parasites and induce at lower doses a chronic infection that can be quantified by brain cyst burden. Here, we show that the mic1-3KO (obtained from type I strain) behaves like type II and III strains, without brain cyst formation. Preliminary results indicate that the i.p. parasitemia with mic1-3KO parasites was 20–50-fold lower than with the control strain 7 d after infection (unpublished data), which suggests a strong defect in infectivity in the peritoneal cavity. Further studies are needed to understand whether the defect in virulence is linked to alteration of invasion of certain cell types present or recruited during infection (20), or to other parameters of infection.

Usually asymptomatic in hosts with intact immunity, toxoplasmosis may lead to severe or lethal damage when associated with immunosuppressive states such as AIDS or when transmitted to the fetus during pregnancy. To date, the only vaccination procedure (in veterinary medicine) uses strains of empirically attenuated parasites lacking the ability to induce chronic infection. The possible reversion to virulent forms of live vaccines requires the development of safer strains by disruption of virulence genes. Our results show that the mic1-3KO might be a promising candidate because mic1-3KO parasites were highly effective in inducing protective immunity in mice and that the persistent parasites in the brain (pseudocysts) in one mouse were not infectious by the oral route (unpublished data), which is required to avoid transmission through consumption of vaccinated animals.

The CBL domain of MIC3: a key domain in toxoplasmosis infection

We have previously characterized the binding properties of MIC3 in vitro and shown that the cell binding site of MIC3 is located in the NH_2-terminal CBL domain (9). Here, we have demonstrated the importance of the domain in toxoplasmosis. This domain was also present in an open reading frame (ORF) of *Eimeria*, another apicomplexa parasite, suggesting that this domain is a fundamental microneme component in *Coccidia*.

We have shown the importance of the two neighboring aromatic residues W126 and F128 in the binding of MIC3 to cells. The nature and spacing of aromatic residues and/or

```
MIC3          -SPSKQETQLCAISSEGKPCRNRQLHTDNG
MIC8          -DPDDENSWLCRISKKYDACGSRE-YSDKG
MIC8-like 1   FQPPSEESWLCRLSTNNGPCSKNSSDPEIG
MIC8-like 2   --PPSDNSWLCRFSFWDGPCVDRQHN-GIG
                * .::: ** :*    .* ...     *

MIC3          YFIGASCPKSACCSKTMCGPGGCG-EFCSS
MIC8          -LKWTFCPEDFCCSKTACFYGSCG-SWCHD
MIC8-like 1   --QWRFCPPGRCCSMSKCGPAGCSIGWCEG
MIC8-like 2   --PWRFCPSGSCCSKVKCAYGSCGGSWCAA
                    ** . ***   *  ..*.  :*

MIC3          NWIFCSSSLIYHPDKSYGG
MIC8          NWALCSSSIIYHDEYSYG-
MIC8-like 1   -WG-NPLCWIKDDTYSDGK
MIC8-like 2   -WN-SGLCVFHNGDYESD-
               *     . : .   . .
```

Figure 5. Alignment of the amino acid sequences of the CBL domain of MIC3, MIC8 (AAK19757), and of putative transmembrane MICs closely related to MIC8 (named MIC8–like 1 and MIC8–like 2) present in the *T. gondii* genome resource (reference 29). Aromatic acids are shown in bold and those involved in cell binding properties of MIC3 are underlined.

other residues is important in defining the binding specificity or affinity of such domains, as shown by the reduced affinity of hevein toward chitin by the single replacement of one tyrosine by phenylalanine (21) or the shift in binding specificity of E-selectin from sialyl-Lewis^x to mannose by substitution of alanine 77 by a lysine residue (22). What remains to be identified is the molecular nature of the cell surface receptor recognized by MIC3. Interestingly, the CBL domain was also described in the *T. gondii* transmembrane MIC, MIC8. It is also found in two ORFs present in the *T. gondii* genome project (Fig. 5) that share all of the characteristics of transmembrane MICs. We have previously shown that recombinant MIC8 can function as adhesin if the protein is dimerized (9) or expressed in conditions of type 1 transmembrane insertion (unpublished data). Interestingly, in these other CBL domain–containing proteins of *T. gondii*, the positions and the type of aromatic residues differ slightly, suggesting that they could recognize different receptors. Having demonstrated the part played by the CBL domain of MIC3 in virulence, we suspect that these homologues may also contribute to virulence by recognizing different cells.

Apicomplexa show a wide range of host cell specificities that can vary at different stages of infection. This specificity may depend on the expression of the MIC repertoire, this latter being highly variable between parasites or between stages of the same parasite. Our data suggest that the MIC repertoire in *T. gondii* is not restricted to the diversity of adhesive domains but may extend polymorphisms into single domains, as exemplified by the MIC3-like family of CBL domains. This diversity may therefore open alternate routes and strengthen the invasive capabilities of *T. gondii* by allowing infection of a wide range of vertebrate hosts and invasion of distinct host cell types at different stages of its developmental cycle.

MATERIALS AND METHODS

Host cell and parasite cultures. All parasites were maintained by serial passage in primary HFFs grown in DMEM (GIBCO BRL) supplemented with 10% FCS and 2 mM glutamine. Mode-K cells (23) were grown in RPMI (Bio-Whittaker) supplemented with 5% FCS, 25 mM Hepes, and 2 mM glutamine. BHK-21 cells (American Type Culture Collection CCL-10) were grown in BHK-21 medium (GIBCO BRL) supplemented with 5% FCS and 2 mM tryptose.

Plasmid constructs. The primers used for constructions were as follows: ML9, 5′-GTGTAAGCTTCAGCGAGTCTCTGAGAG-3′; ML10, 5′-GGGGTACCGAGCTCATGAGCAGAAGCTGCCAG-3′; ML11, 5′-GCACAATTGAGATCTAAAATGCGAGGCGGGACGTCC-3′; ML15, 5′-TGCTATGCATTCCTAGGCTGCTTAATTTTCTCACACGTCAC-3′; ML23, 5′-CTGAATTCAGATCTTACCAGTGTTGGACAAGG-3′; and ML24, 5′-GGGGTACCCCTTGCTAGGTAACCACTCGTGC-3′.

Plasmid pmic3KO-1 was designed to delete the *MIC3* gene in *T. gondii* RH *hxgprt*$^-$ (ΔHX; reference 24) using HXGPRT selection. It was constructed by inserting the 5′ and 3′ flanking region of the MIC3 gene on both sides of the hypoxanthine guanine phosphoribosyl transferase (*HXGPRT*) coding sequence in pminiHXGPRT (24). The 3′ flanking region of the *MIC3* gene (2,514 bp) was PCR amplified from pBlueMIC3 (8) with primers ML9/10 and cloned between the HindIII and KpnI sites of pminiHXGPRT. A 2,135-bp DNA fragment corresponding to the 5′ flanking region of the *MIC3* gene was generated by digestion with the XbaI and NheI of a 3.0-kb EcoRI genomic *MIC3* 5′ fragment (8) and was cloned in the XbaI site of pminiHXGPRT.

Plasmid pmic3KO-2 was designed to delete the *MIC3* gene in *T. gondii* mic1KO using chloramphenicol selection. It was constructed by inserting the 3′ and 5′ flanking regions of *MIC3* on both sides of the *CAT* coding sequence gene in pTUB/CAT (25) using the same restriction sites as described for pminiHXGPRT.

Plasmid pM3MIC3ty was designed to express a COOH-terminal TY-tagged MIC3 protein in mic3KO strain. It was based on plasmid pTUB8mycGFPPftailTY, where the *TUB1* promoter was replaced by the *MIC3* promoter and mycGFPPftail was replaced by the *MIC3* ORF. The promoter region of *MIC3* (562 bp) was PCR amplified from pBlueMIC3 with primers ML23/24 and cloned between KpnI and EcoRI in pTUB8mycGFPPftailTY to give pM3mycGFPPftailTY. The ML24 primer was designed to add the restriction site BglII at the 5′ end upon PCR amplification. The *MIC3* gene was then PCR amplified from pBlueMIC3 with primers ML11/15 and inserted between BglII and NsiI in pM3mycGFPPftailTY to generate pM3MIC3ty.

Plasmid pM3MIC3 was designed to complement the mic1-3KO using phleomycin selection. It was constructed by cloning a 2,072-bp PvuI/SacI fragment of pBlueMIC3, containing the *MIC3* ORF and its 5′ and 3′ flanking regions between SacI and PacI in pT/230-TUB5/BLE.

All constructs were verified by sequencing.

Site-directed mutagenesis. Quickchange (Stratagene), a PCR-based site-directed mutagenesis system, was used to introduce mutations in the *MIC3* gene. For mammalian cell expression, plasmid pOC2 (9) was used as a template for constructing mutants C102G, C107G, C108G, P103A, Y96A, F97A, F121A, W126A, F128A, Y135A, and Y141A. For complementation of mic1-3KO parasites with mutated MIC3, pM3MIC3 was used as a template for constructing mutants W126A, F128A, and Y135A. The presence of the expected mutations was verified by sequencing.

Transfection and selection. Transfections of parasites were conducted as described previously (13). Disruption of the *MIC3* gene in ΔHX and in mic1KO parasites was obtained by electroporation of 100 μg of KpnI-linearized pmic3KO-1 and pmic3KO-2 plasmids, respectively. After overnight growth, transfectants were selected with 25 μg/ml mycophenolic acid and 50 μg/ml xanthine (for HXGPRT selection) or 20 μM chloramphenicol (for CAT selection) for three passages before cloning by limiting dilution

under drug selection. After expanding the clones, KO parasites were identified by IF with anti-MIC3 antibodies (mAb T42F3; reference 26).

Complementation of the mic3KO clone by MIC3ty was obtained by cotransfection using 100 μg pM3MIC3ty and 10 μg pTUB/CAT plasmids and selection with 20 μM chloramphenicol. One-step complementation of the mic1-3KO clone with both MIC1 and MIC3 was obtained by cotransfection using 30 μg pM3MIC3 and 100 μg pM2MIC1myc (13) plasmids and selection with 10 μg/ml phleomycin. Single complementation of mic1-3KO with MIC3 or derivatives W126A, F128A, and Y135A was obtained by transfection using 30 μg pM3MIC3 or mutated pM3MIC3 and selection with phleomycin. Complementations were cloned and verified as described above.

Transient transfection of mammalian cells were conducted as described previously (9).

Immunolocalization experiments. For IF of transfected mammalian cells or intracellular parasites, cell monolayers were washed in PBS and fixed in 4% paraformaldehyde for 20 min. After three washes, cells were permeabilized with 0.1% Triton X-100 in PBS for 10 min, blocked with 10% fetal bovine serum in PBS (PFBS) for 30 min, incubated with primary antibody diluted in 2% PFBS, washed, and then incubated with secondary antibody (FITC goat anti–mouse or Texas red goat anti–rabbit; Sigma-Aldrich).

The coverslips were mounted onto microscope slides using Immunomount (Calbiochem). All observations were performed on a Leica DMRA2 microscope equipped for epifluorescence, and images were recorded with a COOLSNAP CCD camera (Photometrics). Adobe photoshop (Adobe Systems) was used for image processing. When required, matching pairs of images were recorded with the same exposure time and processed identically.

SDS-PAGE, Western blotting, and cell blot assays. SDS-PAGE was performed according to Laemmli et al. (27). Freshly released tachyzoites or transfected cells were boiled in SDS sample buffer with (reduced) or without (nonreduced) 0.1 M dithiothreitol and separated on 10% polyacrylamide gels. Proteins were transferred to nitrocellulose membranes. Western blots were probed as described previously (8) with mAbs anti-MIC3 T4 2F3 or T8 2C10 (1:400), mAb anti-MIC1 T10 1F7 (1:400), mouse anti-V5 (1:5,000; Invitrogen), rabbit anti-MIC8 (1:1,000), rabbit anti-MIC6 (1:1,000), and rabbit anti-MIC4 (1:1,000) followed by goat anti–mouse or goat anti–rabbit IgG alcaline phosphatase conjugates (1:500; Sigma-Aldrich). Cell blot assays were performed as described previously (8).

***Toxoplasma* invasion and attachment assays.** Purified tachyzoites (2×10^5 parasites) were added on confluent HFFs grown on glass coverslips. Cells were fixed 12 h later and stained with eosine-methylene blue (RAL 555). The coverslips were mounted permanently (PERTEX; Microm). The number of vacuoles and tachyzoites per vacuole was counted using a 40× objective.

Red/green invasion assay was performed as described previously (14). In brief, confluent HFF monolayers were infected with 10^7 parasites for 15 min, extensively washed to eliminate unbound parasites, and fixed. Attached parasites were stained with rabbit anti–SAG1 and Texas red goat anti–rabbit, and after subsequent permeabilization with 0.1% Triton X-100, internal parasites were stained with anti-SAG1 mAb (T41E5) and FITC goat anti–mouse. The number of external and internal parasites was counted.

Videomicroscopy. Parasites were grown for 36 h in confluent HFFs cultivated in six-well plates. They were then transferred on the temperature- and atmosphere-controlled stage of an inverted Leica DMIRB microscope equipped with a Micromax CCD camera (Photometrics) driven by Metamorph (Universal Imaging Co.). Egress was induced with 1 μM of calcium ionophore A23187 and motility was recorded at 1 image/2 s. Picture stacks were then analyzed using the pointpicker plug of the imageJ software (http://rsb.info.nih.gov/nih-image) to measure the speed of motion of individual parasites. Four samples of each mutant from two separate experiments were analyzed.

In vivo experiments. 8-wk-old male BALB/C mice (Janvier) housed under approved conditions of the animal research facility at Institut Pasteur de Lille were infected by i.p. injection of 20 tachyzoites freshly harvested from cell culture. Invasiveness of the parasites was evaluated by simultaneous plaque assay of a similar dose of parasites on HFFs. Mouse survival was monitored daily for 40 d, and then weekly. The immune response of surviving animals was tested by Western blotting against RH tachyzoite lysates. Surviving mice that remained seronegative 4 wk after infection, indicating that they had not been infected, were eliminated. Data were represented as Kaplan and Meier plots using GraphPad Prism version 4.00 for Windows (GraphPad Software). Levels of significance were determined with the Logrank test using GraphPad. The protection of surviving mice against *T. gondii* oral cyst challenge was tested on mice that had been infected i.p. for 3 wk with 20 mic1-3KO tachyzoites as described previously (28).

We thank D. Soldati for generous gifts of pM2MIC1myc, pT/230-TUB5/BLE, and pTUB8mycGFPPftailTY plasmids and anti-MIC4, MIC6, and MIC8 antibodies. We thank S. de Rossi (Montpellier Rio Imaging) for help with image acquisition and A. Sahuquet (UMR CNRS 5539) for expert assistance with image analysis. We are grateful to Kai Wengelnick and Robert Menard for helpful discussions. Preliminary genomic DNA sequence data was accessed via http://ToxoDB.org.

Genomic data were provided by The Institute for Genomic Research (supported by the National Institutes of Health grant no. AI05093) and by the Sanger Center (Wellcome Trust). O. Cérède is a recipient of a fellowship from VIHPAL and Fondation pour la Recherche Médicale (FRM). This work was supported by CNRS and a grant from FRM to J.F. Dubremetz.

The authors have no conflicting financial interests.

Submitted: 18 August 2004
Accepted: 19 November 2004

REFERENCES

1. Menard, R. 2001. Gliding motility and cell invasion by Apicomplexa: insights from the *Plasmodium* sporozoite. *Cell. Microbiol.* 3:63–73.
2. Soldati, D., J.F. Dubremetz, and M. Lebrun. 2001. Microneme proteins: structural and functional requirements to promote adhesion and invasion by the apicomplexan parasite *Toxoplasma gondii*. *Int. J. Parasitol.* 31:1293–1302.
3. Tomley, F.M., and D.S. Soldati. 2001. Mix and match modules: structure and function of microneme proteins in apicomplexan parasites. *Trends Parasitol.* 17:81–88.
4. Matuschewski, K., A.C. Nunes, V. Nussenzweig, and R. Menard. 2002. *Plasmodium* sporozoite invasion into insect and mammalian cells is directed by the same dual binding system. *EMBO J.* 21:1597–1606.
5. Kappe, S., T. Bruderer, S. Gantt, H. Fujioka, V. Nussenzweig, and R. Menard. 1999. Conservation of a gliding motility and cell invasion machinery in apicomplexan parasites. *J. Cell Biol.* 147:937–944.
6. Jewett, T.J., and L.D. Sibley. 2003. Aldolase forms a bridge between cell surface adhesins and the actin cytoskeleton in apicomplexan parasites. *Mol. Cell.* 11:885–894.
7. Fourmaux, M.N., A. Achbarou, O. Mercereau-Puijalon, C. Biderre, I. Briche, A. Loyens, C. Odberg-Ferragut, D. Camus, and J.F. Dubremetz. 1996. The MIC1 microneme protein of *Toxoplasma gondii* contains a duplicated receptor-like domain and binds to host cell surface. *Mol. Biochem. Parasitol.* 83:201–210.
8. Garcia-Reguet, N., M. Lebrun, M.N. Fourmaux, O. Mercereau-Puijalon, T. Mann, C.J. Beckers, B. Samyn, J. Van Beeumen, D. Bout, and J.F. Dubremetz. 2000. The microneme protein MIC3 of *Toxoplasma gondii* is a secretory adhesin that binds to both the surface of the host cells and the surface of the parasite. *Cell. Microbiol.* 2:353–364.
9. Cerede, O., J.F. Dubremetz, D. Bout, and M. Lebrun. 2002. The *Toxoplasma gondii* protein MIC3 requires pro-peptide cleavage and dimerization to function as adhesin. *EMBO J.* 21:2526–2536.
10. Shen, Z., and M. Jacobs-Lorena. 1999. Evolution of chitin-binding proteins in invertebrates. *J. Mol. Evol.* 48:341–347.
11. Meissner, M., M. Reiss, N. Viebig, V.B. Carruthers, C. Toursel, S. Tomavo, J.W. Ajioka, and D. Soldati. 2002. A family of transmembrane microneme proteins of *Toxoplasma gondii* contain EGF-like do-

mains and function as escorters. *J. Cell Sci.* 115:563–574.
12. Lourenco, E.V., S.R. Pereira, V.M. Faca, A.A. Coelho-Castelo, J.R. Mineo, M.C. Roque-Barreira, L.J. Greene, and A. Panunto-Castelo. 2001. *Toxoplasma gondii* micronemal protein MIC1 is a lactose-binding lectin. *Glycobiology*. 11:541–547.
13. Reiss, M., N. Viebig, S. Brecht, M.N. Fourmaux, M. Soete, M.M. Di Cristina, J.F. Dubremetz, and D. Soldati. 2001. Identification and characterization of an escorter for two secretory adhesins in *Toxoplasma gondii*. *J. Cell Biol.* 152:563–578.
14. Huynh, M.H., K.E. Rabenau, J.M. Harper, W.L. Beatty, L.D. Sibley, and V.B. Carruthers. 2003. Rapid invasion of host cells by *Toxoplasma* requires secretion of the MIC2-M2AP adhesive protein complex. *EMBO J.* 22:2082–2090.
15. Wright, H.T., G. Sandrasegaram, and C.S. Wright. 1991. Evolution of a family of N-acetylglucosamine binding proteins containing the disulfide-rich domain of wheat germ agglutinin. *J. Mol. Evol.* 33:283–294.
16. Hehl, A.B., C. Lekutis, M.E. Grigg, P.J. Bradley, J.F. Dubremetz, E. Ortega-Barria, and J.C. Boothroyd. 2000. *Toxoplasma gondii* homologue of *Plasmodium* apical membrane antigen 1 is involved in invasion of host cells. *Infect. Immun.* 68:7078–7086.
17. Brecht, S., V.B. Carruthers, D.J. Ferguson, O.K. Giddings, G. Wang, U. Jaekle, J.M. Harper, L.D. Sibley, and D. Soldati. 2000. The *Toxoplasma* micronemal protein MIC4 is an adhesin composed of six conserved apple domains. *J. Biol. Chem.* 276:4119–4127.
18. Reed, M.B., S.R. Caruana, A.H. Batchelor, J.K. Thompson, B.S. Crabb, and A.F. Cowman. 2000. Targeted disruption of an erythrocyte binding antigen in *Plasmodium falciparum* is associated with a switch toward a sialic acid-independent pathway of invasion. *Proc. Natl. Acad. Sci. USA.* 97:7509–7514.
19. Derouin, F., and Y.J.F. Garin. 1991. *Toxoplasma gondii*: blood and tissue kinectics during acute and chronic infections in mice. *Exp. Parasitol.* 73:460–468.
20. Mordue, D.G., and L.D. Sibley. 2003. A novel population of Gr-1+-activated macrophages induced during acute toxoplasmosis. *J. Leukoc. Biol.* 74:1015–1025.
21. Nagahora, H., K. Harata, M. Muraki, and Y. Jigami. 1995. Site-directed mutagenesis and sugar-binding properties of the wheat germ agglutinin mutants Tyr73Phe and Phe116Tyr. *Eur. J. Biochem.* 233:27–34.
22. Kogan, T.P., B.M. Revelle, S. Tapp, D. Scott, and P.J. Beck. 1995. A single amino acid residue can determine the ligand specificity of E-selectin. *J. Biol. Chem.* 270:14047–14055.
23. Vidal, K., I. Grosjean, J.P. Revillard, C. Gespach, and D. Kaiserlian. 1993. Immortalization of mouse intestinal epithelial cells by the SV40-large T gene. Phenotypic and immune characterization of the MODE-K cell line. *J. Immunol. Methods.* 166:63–73.
24. Donald, R.G., and D.S. Roos. 1998. Gene knock-outs and allelic replacements in *Toxoplasma gondii*: HXGPRT as a selectable marker for hit-and-run mutagenesis. *Mol. Biochem. Parasitol.* 91:295–305.
25. Kim, K., D. Soldati, and J.C. Boothroyd. 1993. Gene replacement in *Toxoplasma gondii* with chloramphenicol acetyltransferase as selectable marker. *Science.* 262:911–914.
26. Achbarou, A., O. Mercereau-Puijalon, J.M. Autheman, B. Fortier, D. Camus, and J.F. Dubremetz. 1991. Characterization of microneme proteins of *Toxoplasma gondii*. *Mol. Biochem. Parasitol.* 47:223–233.
27. Laemmli, U.K., F. Beguin, and G. Gujer-Kellenberger. 1970. A factor preventing the major head protein of bacteriophage T4 from random aggregation. *J. Mol. Biol.* 47:69–85.
28. Debard, N., D. Buzoni-Gatel, and D. Bout. 1996. Intranasal immunization with SAG1 protein of *Toxoplasma gondii* in association with cholera toxin dramatically reduces development of cerebral cysts after oral infection. *Infect. Immun.* 64:2158–2166.
29. Kissinger, J.C., B. Gajria, L. Li, I.T. Paulsen, and D.S. Roos. 2003. ToxoDB: accessing the *Toxoplasma gondii* genome. *Nucleic Acids Res.* 31:234–236.